

## High resolution melting curve analysis for rapid detection of severe acute respiratory syndrome coronavirus 2 (SARS-CoV-2) variants

Seyed Jalal Kiani<sup>1</sup>, Mehdi Ramshini<sup>1</sup>, Farah Bokharaei-Salim<sup>1</sup>, Tahereh Donyavi<sup>2</sup>, Babak Eshrati<sup>3</sup>, Majid Khoshmirsafa<sup>4</sup>, Saied Ghorbani<sup>1</sup>, Ahmad Tavakoli<sup>1</sup>, Seyed Hamidreza Monavari<sup>1</sup>, Zohreh Yousefi Ghalejoogh<sup>1</sup>, Mohammad Abbasi-Kolli<sup>5</sup>

<sup>1</sup>Department of Virology, School of Medicine, Iran University of Medical Sciences, Tehran, Iran; <sup>2</sup>Department of Medical Biotechnology, School of Allied Medical Sciences, Iran University of Medical Sciences, Tehran, Iran; <sup>3</sup>Preventive Medicine and Public Health Research Center, Iran University of Medical Sciences, Tehran, Iran; <sup>4</sup>Department of Immunology, School of Medicine, Iran University of Medical Sciences, Tehran, Iran; <sup>5</sup>Department of Medical Genetics, Faculty of Medical Sciences, Tarbiat Modares University, Tehran, Iran

Received June 13, 2022; revised September 25, 2022; accepted February 22, 2023

**Summary.** – Since the emergence of the original Wuhan SARS-CoV-2 strain, several new variants of the virus have emerged. Alpha, Beta, Gamma, Delta and the most recent Omicron variants have been introduced during this pandemic. Several methods including, but not restricted to, allele-specific PCR, ligation with rolling circle amplification and real-time PCR with allele-specific probes are able to detect mutations as low as a single nucleotide polymorphism. High-resolution melting curve analysis is another technique to assess any mutations in a nucleic acid chain. Confirmed samples with SARS-CoV-2 infection were subjected to variant identification using a *de novo*-designed HRM assay. In order to select for mutations with the highest effect on T<sub>m</sub> of the amplicon, deletion mutations of NSP6 (Del 3675-3677), and S1 (Del 144) were chosen for HRM analysis. HRM analysis for the amplicon of the primer set-1 (NSP6) resulted in T<sub>m</sub> differences of -0.39°C, +0.4°C, and -0.6°C between Alpha, Delta, and Omicron variants, respectively, in comparison to the original Wuhan strain. Moreover, HRM analysis of the amplification performed by primer set-2 (S1) led to T<sub>m</sub> differences of +0.32°C, -0.26°C, and +0.24°C between Alpha, Delta, and Omicron variants, respectively, in comparison to original Wuhan strain. The test was able to specify each sample to its variant group with more than 90 percent of confidence. The results obtained in this study demonstrate that using a single closed-tube strategy with a HRM-equipped machine, screening new variants of the virus is possible in a fast and reliable way.

**Keywords:** high resolution melting; SARS coronavirus 2; mutation; variant; genotyping

### Introduction

First detected in Wuhan, China in late 2019, coronavirus disease 2019 (COVID-19) spread rapidly all around the world. Severe acute respiratory virus 2 (SARS-CoV-2), a new member of the *Coronaviridae* family, was introduced as the causative agent of this disease. Transmission of the virus is through the respiratory route and it infects epithelial cells of the respiratory tract. The rapid replication rate of the virus along with its spread to the

E-mail: Kiani.j@iums.ac.ir; phone: +982186703007.

**Abbreviations:** cDNA = complementary DNA; COVID-19 = coronavirus disease 2019; GISAID = Global Initiative on Sharing All Influenza Data; HRM = high resolution melting; RdRP = RNA-dependent RNA polymerase; SARS-CoV-2 = severe acute respiratory syndrome coronavirus 2; SNP = single nucleotide polymorphism; T<sub>m</sub> = melting temperature; VOC = variant of concern; VTM = virus transport medium

lower respiratory tract system are among the reasons for poor prognosis (Cao *et al.*, 2020).

Viral RNA-dependent RNA polymerase (RdRP) generates some errors while making full-length RNA copies of the long genome of SARS-CoV-2 (~30 kb) and thus mutant strains appear. SARS-CoV-2 RdRP has a proofreading activity to some extent. However, because of the rapid replication rate of the virus in the host cells and also due to immune response selection pressures, especially in regions exposed to antibodies, rates of mutation accumulation increase (Castro *et al.*, 2005).

Following the first cases of the infection in Wuhan, several other variants have appeared, some of which are variants of concern (VOC). These VOCs include Alpha (B.1.1.7 lineage; first reported in the UK), Beta (B.1.351 lineage; South Africa), Gamma (B.1.1.28 lineage; first reported in Brazil), Delta (B.1.617.2 lineage; first reported in India), and the most recent Omicron (B.1.1.529 lineage; first reported in South Africa) (WHO, 2022). Table 1 summarizes the most important mutations that are characteristic of each variant (ViralZone, 2022). Although other nucleotide substitutions may exist in different variants, detection of these mutations is sufficient to specify a virus as a specific variant.

Different mutation detection methods are available (Metzker, 2010). These methods include conventional

Maxam-Gilbert and Sanger sequencing, and Shotgun sequencing. Besides, high-throughput sequencing methods such as single-molecule real-time sequencing, pyrosequencing, sequencing by synthesis (Illumina), and nanopore sequencing, are available as well. While these methods determine full length nucleotide chain of a sequence of interest, mutations can also be detected in a specific location indirectly. Allele-specific PCR, allele-specific primer extension, ligation with rolling circle amplification, and real-time PCR with allele-specific probes, which are able to detect single nucleotide polymorphisms (SNPs) are some of the indirect mutation analysis methods that have been developed (Slatko *et al.*, 2018).

In addition to the above-mentioned methods, high-resolution melting curve analysis (HRM) of the PCR product can help identify mutations in an array of nucleic acid residues. The basics of this method are that any changes/ variations in the DNA sequence will result in changes in the melting temperature ( $T_m$ ) of the intended PCR product. Any differences in  $T_m$ , including as low as just one nucleotide substitution and/or deletion, are monitored and demonstrated in high resolution by any real-time PCR machine capable of performing HRM (Montgomery *et al.*, 2007). Deletions or substitutions of any C/G with A/T will result in lower  $T_m$ , while substitutions of A/T with C/G or

**Table 1. World Health Organization (WHO) announced variants of concern (VOC)**

Lineage	Synonyms	Emergence	Spike mutations	Other mutations
Alpha	B.1.1.7	UK, Sep 2020	<b>Del 69-70; Del 144;</b> N501Y; A570D; D614G; P681H; T716I; S982A; D1118H	<b>ORF1ab:</b> T1001I; A1708D; I2230T; <b>Del 3675-3677</b> <b>ORF8:</b> R52I; Q27*; Y73C; S84L <b>N:</b> D3L; R203K; G204R; S235F
Beta	B.1.351	South Africa, Aug 2020	L18F; <b>D80A;</b> D215G; Del 241-243; K417N; E484K; N501Y; D614G; A701V	<b>E:</b> P71L <b>N:</b> T205I <b>ORF1a:</b> T265I; K1655N; K3353R; <b>Del 3675-3677</b> <b>ORF3a:</b> Q57H; S171L <b>ORF8:</b> S84L
Gamma	B.1.1.28.1	Brazil, Jul 2020	L18F; T20N; P26S; D138Y; R190S; K417N/T; E484K; N501Y; D614G; H655Y; T1027I; V1176F	<b>ORF1ab:</b> S1188L; K1795Q; Del 3675-3677 <b>ORF3a:</b> S253P <b>ORF8:</b> S84L; E92K <b>N:</b> P80R; R203K; G204R
Delta	B.1.617.2	India, Dec 2020	T19R; <b>G142D; E156G; Del 157-158;</b> L452R; T478K; D614G; P681R; D950N	<b>ORF1a:</b> A1306S; P2046L; P2287S; V2930L; T3255I; T3646A <b>nsp3:</b> P1469S <b>nsp12:</b> P323L, G671S <b>nsp13:</b> P77L <b>ORF3a:</b> S26L <b>M:</b> I82T <b>ORF7a:</b> V82A, T120I <b>N:</b> D63G, R203M, G215C; D377Y <b>ORF8:</b> S84L, Del 119-120
Omicron BA.1	B.1.1.529	South Africa, Dec 2021	A67V; <b>Del 69-70;</b> T95I; <b>GVVY142-145D;</b> NL211-212I ins214EPE; G339D; S371L; S373P; S375F; K417N; N440K; G446S; S477N; T478K; E484A; Q493R; G496S; Q498R; N501Y; Y505H; T547K; D614G; H655Y; N679K; P681H; N764K; D796Y; N856K; Q954H; N969K; L981F	<b>N:</b> P13L; Del 31-33, R203K, G204R <b>ORF1ab:</b> K856R, SL2083-2084I, A2710T, T3255I, P3395H, <b>Del 3674-3676,</b> I3758V, P4715L, I5967V <b>E:</b> T9I <b>M:</b> D3G, Q19E, A63T <b>Orf9b:</b> P10S, 27-29del <b>ORF8:</b> S84L

insertions will cause higher  $T_m$  of the PCR product. One of the important factors for a successful HRM analysis is to shorten the amplification target as much as possible. It is shown that HRM works better if the amplification target length ranges between 65 and 300 bp. One of the advantages of this method is that any variations in the intended target can be analyzed in a short amount of time without using complicated instruments or expensive fluorescently labeled oligonucleotide probes. Even though HRM analysis has to be confirmed by sequencing, the method can be used for fast screening of the variations in a specific sequence of interest (Reed *et al.*, 2007).

Considering the importance of surveillance of mutations in SARS-CoV-2, which might be associated with higher/lower morbidity and mortality, the aim of the current study was to evaluate the application of HRM analysis to screen for mutations related to different variants of SARS-CoV-2. This can provide us with a rapid screening method for identification of mutations in the virus genome.

## Materials and Methods

**Ethical approval.** This study was assessed and approved by the Research Ethics Committee of Iran University of Medical Sciences (ID: IR.IUMS.REC.1400.175). An informed consent was signed by the participants in the study.

**Patient samples.** Sixteen naso/oropharyngeal swab samples were taken from patients referred to the West Health Center of Tehran, affiliated with the Iran University of Medical Sciences. The samples were collected in the viral transport medium (VTM) and stored at 4°C until use.

**Viral RNA extraction.** Viral genomic RNA extraction was performed with a commercial viral RNA extraction kit (RNJia Virus Kit; ROJE Technologies Corporation), according to the manufacturer's instructions. The extracted RNA was eluted in 50 µl of elution buffer provided in the kit and stored at -20°C for further analysis.

**Real-time PCR for the detection of SARS-CoV-2.** Detection of the virus was performed with a commercial SARS-CoV-2 detection kit (COVID-19 One-Step RT-PCR; Pishtazteb Diagnostics) based on its instructions for use. This kit detects parts of ORF1ab and N genes as viral target genes and RNase P as the internal control. Briefly, for each reaction, 9 µl of the enzyme mix was mixed with 1 µl of primer-probe mixture. Five microliters of nuclease-free water and 5 µl of the extracted viral RNA were also added to the mixture. The thermal cycling profile of the real-time PCR was as follows: reverse transcription at 50°C for 20 min, initial denaturation at 95°C for 3 min, 45 cycles of denaturation at 95°C for 10 s and annealing/extension at 55°C for 40 s. Data acquisition was scheduled at the end of annealing/extension step for green (ORF1ab), Yellow (N), and Orange

(RNase P) channels. Amplification curves with cycle threshold (Ct) of not more than 40 were considered as true amplification (positive).

**Real-time PCR for the detection of SARS-CoV-2 variants.** Detection of known SARS-CoV-2 variants was performed using a commercial kit (GenovA SARS-CoV-2 OneStep RT-PCR Kit; Bioluence), according to the manufacturer's instructions. The kit detects viral ORF1a, N, and S regions in addition to RNase P as the internal control. Mutations in different variants of the virus results in different combination of fluorescent signals and the results are interpreted based on the kit manual (FAM for Alpha; FAM-TEXAS Red for Beta/Gamma/Lambda; FAM-Cy5 for Omicron; FAM-TEXAS Red-Cy5 for Delta). Briefly, 10 µl of the mastermix was mixed with 10 µl of the extracted RNA. The following temperature profile was applied on the Qiagen Rotor Gene Q machine: reverse transcription at 53°C for 15 min, initial denaturation at 95°C for 3 min, 46 cycles of denaturation at 93°C for 5 s and annealing-extension at 60°C for 25 s. Data collection was programmed at the end of annealing-extension step for green (FAM), yellow (HEX), orange (TEXAS Red), and red (Cy5) channels. The Ct of less than 40 was considered as true amplification (positive).

**Primer design for HRM analysis.** The most important mutations of SARS-CoV-2 variants are summarized in Table 1. Deletion mutations of NSP6 (Del 3675-3677), S1 (Del 144), and S2 (Del 69-70) were chosen for HRM analysis since it was expected that deletion mutations would have the highest effect on  $T_m$  of the amplicon and contribute to easier identification of variants. The primers were designed using Primer-BLAST online software. Important criteria for HRM primer design include amplicon length between 80 to 150 bp, GC content of 40-60%,  $T_m$  difference of less than 1°C for forward and reverse primers, and the absence of other mutations in the amplicon region. Selected primers were analyzed for secondary structures and primer dimer formation using OligoAnalyser Tool (Integrated DNA Technologies; USA). The most appropriate annealing temperature was selected based on the performance of the primers in a gradient PCR assay. The efficiency of the reaction was also evaluated using serial dilutions of a known sample. The primer sequences and the amplicon size of each primer pair are shown in Table 2.

**Complementary DNA (cDNA) synthesis.** Samples of patients with confirmed SARS-CoV-2 infection were subjected to cDNA synthesis. Ten microliters of the extracted viral RNA were used as the template. Sequence-specific primers were used with a commercial cDNA synthesis kit (Superscript cDNA synthesis kit; ThermoFisher Scientific) according to the instructions of the manufacturer. Briefly, 4 µl of 5X RT buffer solution, 0.2 mM dNTP mix, 0.5 µl of RNaseOUT, 0.5 µl of Moloney Murine Leukemia Virus Reverse Transcriptase (M-MLV RT) enzyme, and 1 µl of nuclease-free water were mixed with 0.5 µM of forward and reverse primers to the final volume of 20 µl and incubated at 42°C for 30 min. Enzyme inactivation was achieved by in-

**Table 2. Primer sequences used for the high resolution melt curve analysis (HRM)**

Primers	Target	Amplicon size	Primer	Sequence	Start	Stop	Tm
Primer set-1	NSP6	118 bp	Forward	TGCGTATTATGACATGGTTGGA	11247	11247	58.52
			Reverse	ACAGTTCTTGCTGTCATAAGGA	11364	11343	58.04
Primer set-2	S-1	138 bp	Forward	AGACCCAGTCCCTACTTATTGT	21900	21921	58.61
			Reverse	CTCTGAACCTCACTTCCATCCA	22037	22016	58.39
Primer set-3	S-2	105 bp	Forward	ACTCAGGACTTGTTCTTACCTT	21713	21734	57.35
			Reverse	TGGTAGGACAGGGTTATCAAAC	21817	21796	58.11

cubation of the reaction mix at 70°C for 10 min. Samples were preserved at -20°C until further analysis.

**HRM analysis.** HRM analysis was performed with a pre-amplification step using each primer pair on the Qiagen Rotor-Gene Q5plex HRM Platform (QIAGEN GmbH, Hilden, Germany). The reaction mixture contained HOT FIREPol EvaGreen HRM Mix (Solis BioDyne), 0.5 µM forward and 0.5 µM reverse primers (10 pmol), and nuclease-free water. The amplification step included a 12-min hold at 95°C for enzyme activation and 40 cycles of 10 s denaturation at 95°C and 15 s annealing/extension at 57°C. Data acquisition was scheduled at the end of the annealing/extension step for the green channel. Moreover, the HRM step was programmed after the amplification step with the following settings: a pre-hold step at 50°C for 90 s, HRM analysis at a range of 70–85°C, temperature increment of 0.1°C, and a hold of 2 s/step. Each experiment was performed at least in duplicate. For HRM data analysis, only samples with a Ct of not more than 30 were included, because late amplifications may be an indication of not reaching the reaction plateau and may result in affected HRM resolution due to lower overall fluorescence. Moreover, samples with higher Ct than rest of the group will result in Tm shift and may affect final interpretations.

## Results

### *Detection of SARS-CoV-2 by multiplex real-time PCR*

A multiplex real-time PCR assay was used for the detection of SARS-CoV-2 target genes (ORF1ab and N) as well as

the internal housekeeping gene (RNase P) in the samples (data not shown).

### *Detection of SARS-CoV-2 variants*

The selected positive samples were tested for known SARS-CoV-2 variants using a commercial kit. The results were interpreted based on the kit instructions. Briefly, amplification curve on the green (FAM) channel represented the alpha variant. Amplification curves both on the green (FAM) and orange (TEXAS Red) channels represented either beta, gamma, or lambda variants. Amplification curves on green (FAM), orange (TEXAS Red), and red (Cy5) channels showed the delta variant. Amplification curves on the green (FAM) in addition to the red (Cy5) channels were indicative of the omicron variant presence (Supplementary Fig. 1). The results were confirmed by Sanger sequencing at a reference laboratory (Pasteur Institute of Iran, Tehran, Iran).

### *High-resolution melt curve analysis*

Three primer sets were designed for HRM analysis of mutations in the genome of different SARS-CoV-2 variants. Multiple sequence alignment of different amplicons is shown in Fig. 1. Expected mutations in the amplicons of the primer sets are summarized in Table 3.

In the first step, the function of the primer sets in distinguishing the Alpha variant from the original Wuhan strain was evaluated (Fig. 2). The results showed that

**Table 3. Expected mutations in the amplicons of 3 primer sets**

	Wuhan	Alpha (UK)	Beta	Delta	Omicron BA.1
Primer set-1	NSP6	- del 3674-3676 (TCTGGTTTT)	- del 3674-3676 (TCTGGTTTT)	- A > G	- del 3674-3676 (TCTGGTTTT) - G > T
Primer set-2	S 144	- del Y 144 (TTA)	None	- G > A - G > T - C > T - A > T	- G V Y Y 142-145 D (TGTTTATTA)
Primer set-3	S 69-70	- del 69-70 (ACATGT)	- A > C	None	- del 69-70 (ACATGT) - C > A

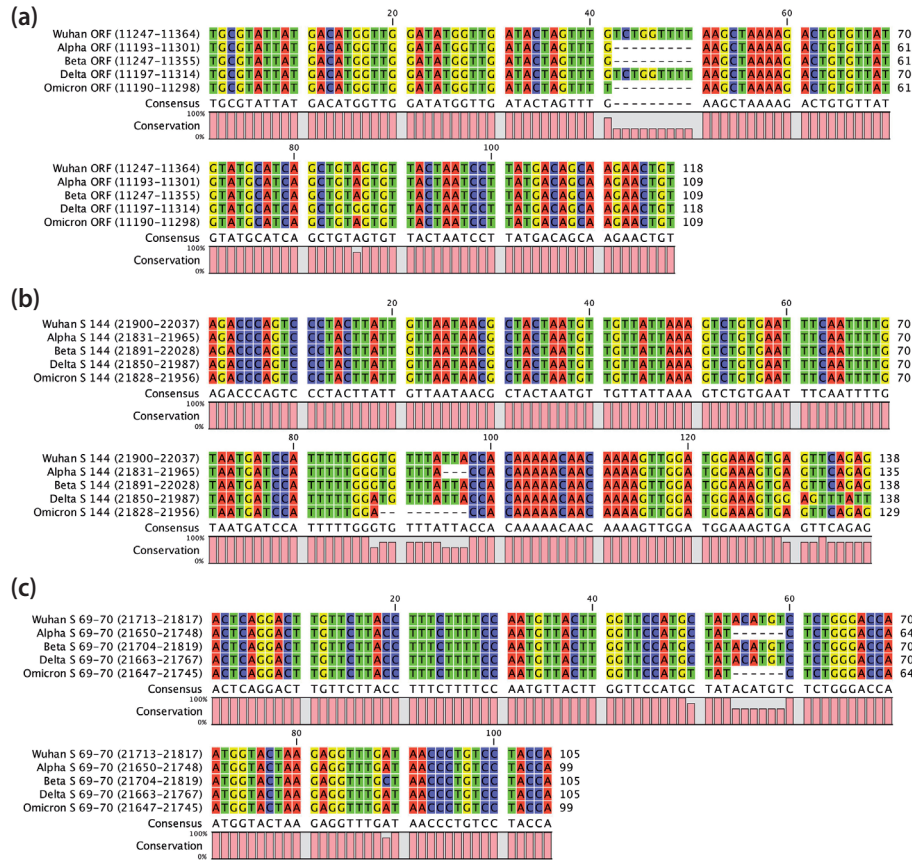


Fig. 1

### Multiple sequence alignment of the selected SARS-CoV-2 variants

The amplicon sequences of the target regions for the primer set-1 (a), primer set-2 (b), and primer set-3 (c) were subjected to multiple alignment using CLC sequence viewer-7 software. (Acc. Nos. for the reference sequences in GenBank: Wuhan NC\_045512; Alpha MZ344997; Beta MW598419; Delta MZ359841; Omicron OL672836).

primer set-1 (NSP6) produced a  $T_m$  difference of  $0.35^\circ\text{C}$  between the Wuhan strain and the Alpha variant. Primer set-2 (S1) also detected a  $T_m$  difference of  $0.23^\circ\text{C}$  between the Wuhan strain and the Alpha variant. However, primer set-3 (S2) did not result in a significant difference in  $T_m$  ( $0.08^\circ\text{C}$ ) to distinguish the Alpha variant from the Wuhan strain. Therefore, primer set-1 and primer set-2 were selected for subsequent experiments.

Then, the selected primer sets were used for the detection of the Alpha, Delta, and Omicron variants from the original strain (Fig. 3). HRM analysis of the amplicon of the primer set-1 (NSP6) showed  $T_m$  differences of  $-0.39^\circ\text{C}$ ,  $+0.4^\circ\text{C}$ , and  $-0.6^\circ\text{C}$  between Alpha, Delta, and Omicron variants, respectively, in comparison with the original Wuhan strain (Fig. 3a). Moreover, HRM analysis of the amplification performed using primer set-2 (S1) showed  $T_m$  differences of  $+0.32^\circ\text{C}$ ,  $-0.26^\circ\text{C}$ , and  $+0.24^\circ\text{C}$  between Alpha, Delta, and Omicron variants, respectively, in comparison to original Wuhan strain (Fig. 3b). Efficiency of

the reactions was also evaluated using serial dilutions of a known sample and it was 93% for primer set-1 and 94% for primer set-2.

The results of the present study showed that both primer sets were able to distinguish selected viral variants with a confidence of more than 90% (Fig. 4). Comparing the suitability of the designed HRM assay for variant detection with the results of Sanger sequencing revealed that both primer sets correctly identified the variant of 14/16 (87.5%) samples.

## Discussion

High-resolution melting curve analysis is a simple method for genotyping, mutation scanning and sequence matching, which does not require any further sample processing (Liew *et al.*, 2004; Montgomery *et al.*, 2007). Following PCR amplification, melting curves of

PCR products are analyzed by tracking the fluorescence emission of a saturating double-stranded DNA binding dye. As the temperature is raised, the fluorescence emission decreases. As low as one nucleotide pair variation between two nucleotide arrays will cause alterations in the melting temperature of the amplicons (Rouleau *et al.*, 2009; Al-Koofee *et al.*, 2019). HRM is a closed-tube method for fast, accurate, and high throughput mutation screening at a lower cost than many other alternatives (Al-Koofee *et al.*, 2019). The results of the present study showed that by targeting a short amplicon containing a mutation of interest, different variants of SARS-CoV-2 can be distinguished. Nucleotide changes in the amplified targets within NSP6 and S regions induced enough differences in  $T_m$  of the amplicons to be analyzed by HRM software and specify each sample into its variant group with

more than 90 percent of confidence. Other researchers also used this technique for differentiating SARS-CoV-2 variants. For instance, Aoki *et al.* (2021) demonstrated that HRM analysis can be used for the identification of five mutations as known strain determinants of Global Initiative on Sharing All Influenza Data (GISAID) clades (L, S, V, G, GH, and GR). Their results also showed that the RNA template (after cDNA synthesis) and saliva sam-

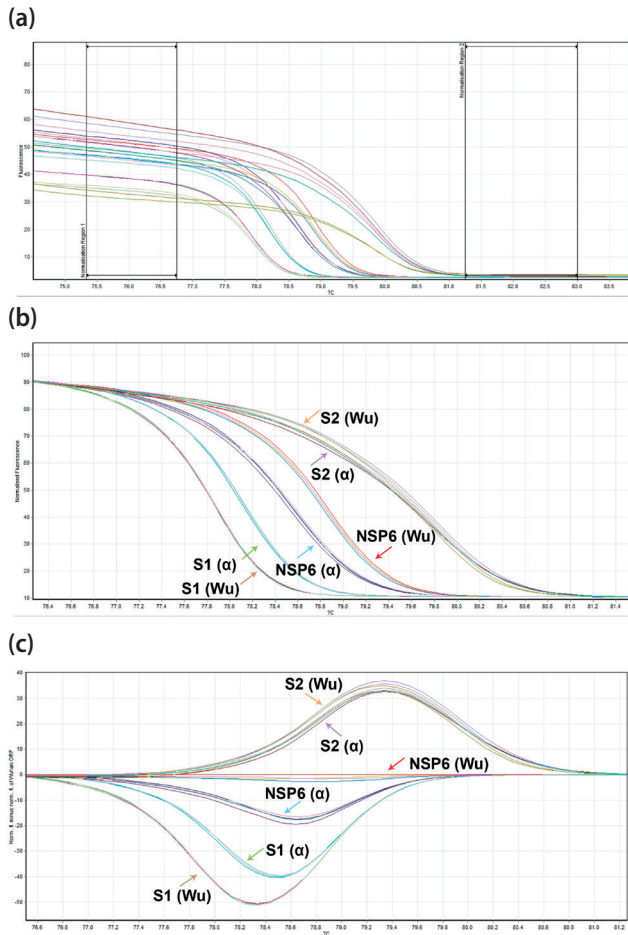


Fig. 2

**Application of three primer sets to distinguish between the Wuhan strain and the Alpha variant**

(a) DNA melt curves for the amplicons of three primer sets (NSP6, S1, S2) and their normalization regions. (b) Normalized graphs of melt curve analysis for NSP6, S1, and S2 amplicons. (c) Difference graph representation of melt curve analysis for NSP6, S1, and S2 amplicons.

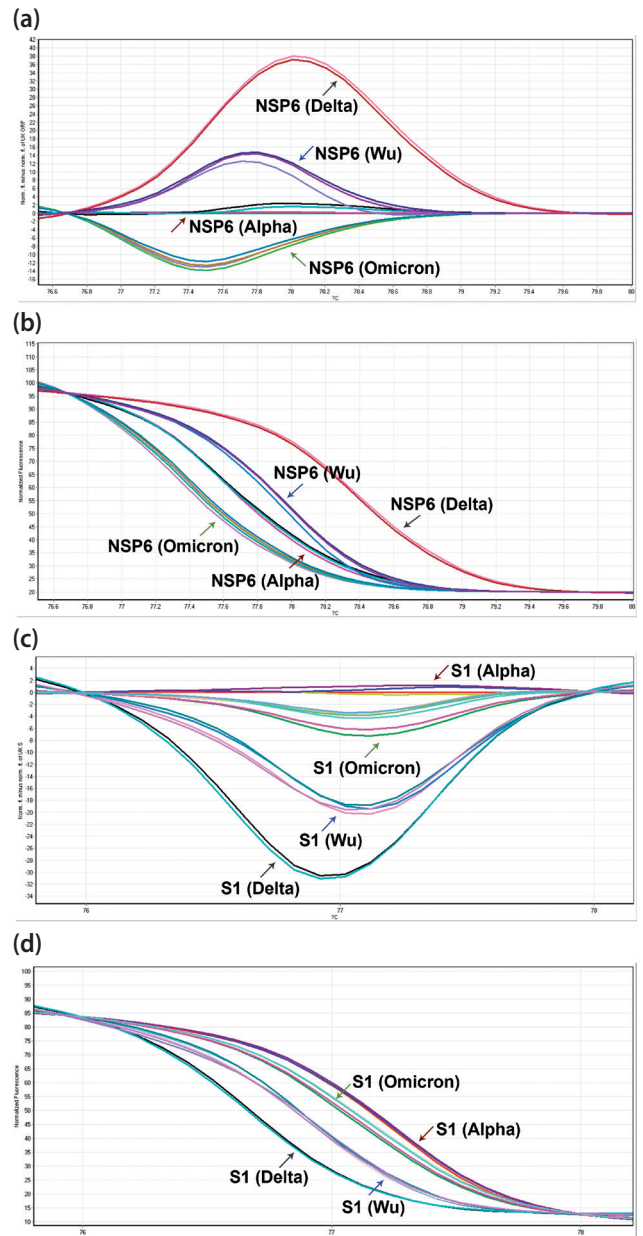


Fig. 3

**Differentiation of SARS-CoV-2 variants by HRM analysis**

Melt curve analyses of the amplicons are illustrated with normalized graph and difference graph representations for primer set-1 (a and b) and primer set-2 (c and d).

(a)

No.	C	Name	Genotype	Confidence %
41		34411-1 (O-UK)	UK ORF	100.00
42		34411-2 (O-UK)	UK ORF	99.96
43		34375-1 (O-UK)	UK ORF	96.22
44		34375-2 (O-UK)	UK ORF	98.22
47		5175-1 (O-Wu)	Wu ORF	87.46
48		5175-2 (O-Wu)	Wu ORF	93.96
49		66846-1 (O-Omi)	Omicron ORF	99.72
50		66846-2 (O-Omi)	Omicron ORF	91.36
51		66848-1 (O-De)	Delta ORF	100.00
52		66848-2 (O-De)	Delta ORF	98.09
53		66861-1 (O-Om)	Omicron ORF	100.00
54		66861-2 (O-Om)	Omicron ORF	98.48
55		66879-1 (O-Om)	Omicron ORF	97.84
56		66879-2 (O-Om)	Omicron ORF	99.12
57		Wuhan PC O-1	Wu ORF	100.00
58		Wuhan PC O-2	Wu ORF	98.89

(b)

No.	C	Name	Genotype	Confidence %
1		34411-1 (S-UK)	UK S	100.00
2		34411-2 (S-UK)	UK S	99.89
3		34375-1 (S-UK)	UK S	99.47
4		34375-2 (S-UK)	UK S	98.77
5		5626-1 (S-Wu)	Wu S	97.49
6		5626-2 (S-Wu)	Wu S	96.82
9		66846-1 (S-Omi)	Omicron S	89.88
10		66846-2 (S-Omi)	Omicron S	94.04
11		66848-1 (S-De)	Delta S	100.00
12		66848-2 (S-De)	Delta S	99.34
13		66861-1 (S-Om)	Omicron S	100.00
14		66861-2 (S-Om)	Omicron S	99.81
15		66879-1 (S-Om)	Omicron S	99.30
16		66879-2 (S-Om)	Omicron S	99.91
17		Wuhan PC S-1	Wu S	100.00
18		Wuhan PC S-2	Wu S	98.92

Fig. 4

## HRM analysis results table

The application of primer set-1 (a) and primer set-2 (b) resulted in variant differentiation with a confidence of more than 90%.

ples were suitable for this analysis and did not have any negative impacts on the test. In another study, Aoki and colleagues successfully used this technique to screen for L452R and T478K spike mutations in Delta variant (Aoki *et al.*, 2021). Diaz-Garcia *et al.* (2021) applied this method for genotyping of the major SARS-CoV-2 clade at the time of their study. They reported that a short-amplicon HRM assay can be used to specifically detect variations in position 417 of the receptor binding domain of the spike protein. Earlier denaturation in the melting pattern of the PCR product was shown in the GR clade compared to the non-GR samples with later denaturation. (Diaz-Garcia *et al.*, 2021). In order to demonstrate D614G mutation in the S gene, Gazali *et al.* (2021) developed a qPCR-HRM assay using an amplicon of 172 bp in length and a  $T_m$  difference of 0.23 °C between D614 and G614 variants. They suggested that this assay can be considered as a powerful tool for high-throughput screening and epidemiological studies of circulating variants (Gazali *et al.*, 2021). Our primary hypothesis was that deletion mutations will result in lower  $T_m$  of the amplicon of interest and this was proved by the melting curve analysis of the ORF PCR product. However, in the case of primer set-2 amplicon, deletion of TTA in Alpha variant and TGTTTATTA in Omicron variant resulted in higher  $T_m$  of the PCR product, which is associated with higher GC content of the amplicon (138 nt, 32.6% GC,  $T_m$  87.1°C for Wuhan; 135 nt, 33.3% GC,  $T_m$  87.5°C for Alpha, 138 nt, 30.4% GC,  $T_m$  86.2°C for Delta, and 129 nt, 33.3% GC,  $T_m$  87.3 for Omicron).

The emergence of new SARS-CoV-2 variants, especially VOCs with significant differences in morbidity and/or mortality rate, necessitates screening for known and new variants of SARS-CoV-2. Common methods for the detection of different variants are direct sequencing,

next-generation sequencing, fluorescent probe-based real-time PCR assays, and so forth. However, these techniques take considerable time and effort, rely on expensive fluorescently-labeled probes, and may not be suitable for high-throughput screening of mutations.

The inexorable occurrence of mutations during rapid replication of the virus is associated with the emergence of new VOCs. Subsequent to the BA.1 subvariant of Omicron, other subvariants including BA.2, BA.2.12.1, BA.2.75, BA.4, and BA.5 have been responsible for the spread of the ongoing pandemic. Multiple sequence alignment of the NSP6 amplicon (primer set-1) showed that BA.1 differs only in one nucleotide (T instead of G) compared to all other subvariants (Supplementary Fig. 2). However, considering the absence of BA.1 DEL144 in all other subvariants, it seems that primer set-2 can be used more efficiently to differentiate BA.1 from the others. Albeit two nucleotide substitutions (A>G and T>C) would potentially modify the pattern of BA.2.75 melting curves in comparison with other subvariants (Supplementary Fig. 2). Regarding primer set-3 (S2), although our results revealed that it is not capable to efficiently differentiate between Wuhan and Alpha variants, *in-silico* analyses imply that, due to the presence of DEL69-70, the test would be able to distinguish between BA.4/5 and all BA.2s (BA.2, BA.2.12.1, BA.2.75), which is of importance for current situation of the pandemic (Supplementary Fig. 2). Further wet lab experiments are required to support this hypothesis.

One limitation of the present study was that each one of the proposed primer sets was incapable to distinguish the Beta variant of the virus, individually. Although the Beta variant contains NSP6 del 3674-3676 (primer set-1) similar to Alpha, and lacks S del Y144 (primer set-2) similar to Delta, simultaneous interpretation of the results

for both primer sets is required to allocate one sample to the category of this variant. Therefore, we decided not to include this variant in our represented findings. Another important limitation was the small sample size used for method development and evaluation. However, considering the use of Sanger-sequenced samples as reliable representatives of each variant and the obtained notable results, the proposed method can be considered as a preliminary promising finding for further investigations in future.

The results obtained in this study demonstrated that HRM, as a single closed-tube method, makes it possible to screen for new variants of the virus in a fast and reliable way. However, one of the concerns regarding the application of HRM analysis for mutation detection is that any changes in the amplicon will result in  $T_m$  differences. This may confound the interpretation of the results. Therefore, it is highly recommended that the results be confirmed by direct sequencing as the gold standard method.

### Conclusion

High-resolution melting curve analysis is a method to provide a rapid mutation screening. Although this strategy has been mostly used for double-stranded DNA sequence assessment, the present study supports the application of HRM analysis for RNA sequence mutation screening. The latter is of importance for the detection of different viral variants as well as drug-resistance mutations in several virus families.

**Acknowledgments.** The authors would like to thank all the members of the Molecular diagnostics laboratory of Iran University of Medical Sciences located in the West Health Center of Tehran. This project was supported financially by the Iran University of Medical Sciences (grant No. 19730).

**Supplementary information** is available in the online version of the paper.

### References

- Al-Koofee DA, Ismael JM, Mubarak SM (2019): Point mutation detection by economic HRM protocol primer design. *Biochem. Biophys. Rep.* 18, 100628. <https://doi.org/10.1016/j.bbrep.2019.100628>
- Aoki A, Adachi H, Mori Y, Ito M, Sato K, Okuda K, Sakakibara T, Okamoto Y, Jinno H (2021): A rapid screening assay for L452R and T478K spike mutations in SARS-CoV-2 Delta variant using high-resolution melting analysis. *J. Toxicol. Sci.* 46(10), 471-476. <https://doi.org/10.2131/jts.46.471>
- Aoki A, Mori Y, Okamoto Y, Jinno H (2021): Development of a genotyping platform for SARS-CoV-2 variants using high-resolution melting analysis. *J. Infect. Chemother.* 27(9), 1336-1341. <https://doi.org/10.1016/j.jiac.2021.06.007>
- Cao Y, Cai K, Xiong L (2020): Coronavirus disease 2019: A new severe acute respiratory syndrome from Wuhan in China. *Acta Virol.* 64(2), 245-250. <https://doi.org/10.4149/av.2020.201>
- Castro C, Arnold JJ, Cameron CE (2005): Incorporation fidelity of the viral RNA-dependent RNA polymerase: a kinetic, thermodynamic and structural perspective. *Virus Res.* 107(2), 141-149. <https://doi.org/10.1016/j.virusres.2004.11.004>
- Diaz-Garcia H, Guzmán-Ortiz AL, Angeles-Florianio T, Parra-Ortega I, López-Martínez B, Martínez-Saucedo M, Aquino-Jarquín G, Sánchez-Urbina R, Quezada H, Granados-Riveron JT (2021): Genotyping of the Major SARS-CoV-2 Clade by Short-Amplicon High-Resolution Melting (SA-HRM) Analysis. *Genes* 12(4), 531. <https://doi.org/10.3390/genes12040531>
- Gazali FM, Nuhamunada M, Nabilla R, Supriyati E, Hakim MS, Arguni E, Daniwijaya EW, Nuryastuti T, Haryana SM, Wibawa T, Wijayanti N (2021): Detection of SARS-CoV-2 spike protein D614G mutation by qPCR-HRM analysis. *Heliyon* 7(9), e07936. <https://doi.org/10.1016/j.heliyon.2021.e07936>
- Liew M, Pryor R, Palais R, Meadows C, Erali M, Lyon E, Wittwer C (2004): Genotyping of Single-Nucleotide Polymorphisms by High-Resolution Melting of Small Amplicons. *Clin. Chem.* 50(7), 1156-1164. <https://doi.org/10.1373/clinchem.2004.032136>
- Metzker ML (2010): Sequencing technologies-the next generation. *Nat. Rev. Genet.* 11(1), 31-46. <https://doi.org/10.1038/nrg2626>
- Montgomery J, Wittwer CT, Palais R, Zhou L (2007): Simultaneous mutation scanning and genotyping by high-resolution DNA melting analysis. *Nat. Protoc.* 2(1), 59-66. <https://doi.org/10.1038/nprot.2007.10>
- Reed GH, Kent JO, Wittwer CT (2007): High-resolution DNA melting analysis for simple and efficient molecular diagnostics. *Pharmacogenomics*, 8(6), 597-608. <https://doi.org/10.2217/14622416.8.6.597>
- Rouleau E, Lefol C, Bourdon V, Coulet F, Noguchi T, Soubrier E, Bieche I, Olschwang S, Sobol H, Lidereau R (2009): Quantitative PCR high-resolution melting (qPCR-HRM) curve analysis, a new approach to simultaneously screen point mutations and large rearrangements: application to MLH1 germline mutations in Lynch syndrome. *Hum. Mutat.* 30(6), 867-875. <https://doi.org/10.1002/humu.20947>
- Slatko BE, Gardner AF, Ausubel FM (2018): Overview of next-generation sequencing technologies. *Curr. Protoc. Mol. Biol.* 122(1), e59. <https://doi.org/10.1002/cpmb.59>
- ViralZone (2022): SARS-CoV-2 circulating variants. from <https://viralzone.expasy.org/9556>.
- World Health Organization (2022): Tracking SARS-CoV-2 variants. from <https://www.who.int/en/activities/tracking-SARS-CoV-2-variants>.



## SUPPLEMENTARY INFORMATION

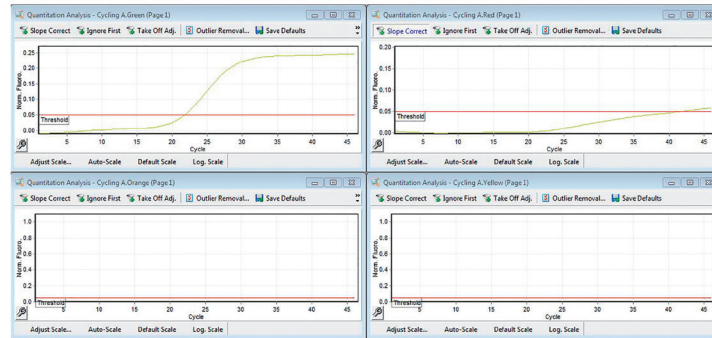
### **High resolution melting curve analysis for rapid detection of severe acute respiratory syndrome coronavirus 2 (SARS-CoV-2) variants**

Seyed Jalal Kiani<sup>1</sup>, Mehdi Ramshini<sup>1</sup>, Farah Bokharaei-Salim<sup>1</sup>, Tahereh Donyavi<sup>2</sup>, Babak Eshrati<sup>3</sup>, Majid Khoshmirsafa<sup>4</sup>, Saied Ghorbani<sup>1</sup>, Ahmad Tavakoli<sup>1</sup>, Seyed Hamidreza Monavari<sup>1</sup>, Zohreh Yousefi Ghalejoogh<sup>1</sup>, Mohammad Abbasi-Kolli<sup>5</sup>

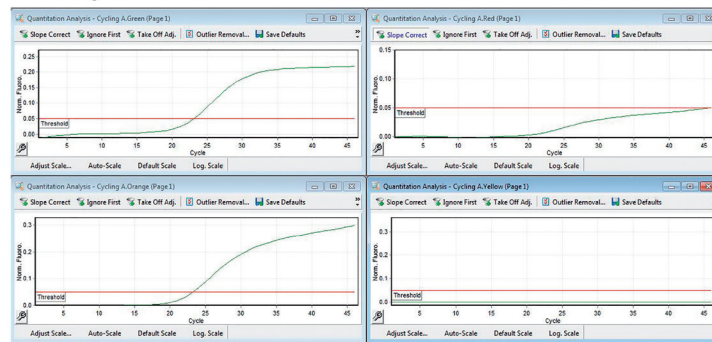
<sup>1</sup>Department of Virology, School of Medicine, Iran University of Medical Sciences, Tehran, Iran; <sup>2</sup>Department of Medical Biotechnology, School of Allied Medical Sciences, Iran University of Medical Sciences, Tehran, Iran; <sup>3</sup>Preventive Medicine and Public Health Research Center, Iran University of Medical Sciences, Tehran, Iran; <sup>4</sup>Department of Immunology, School of Medicine, Iran University of Medical Sciences, Tehran, Iran; <sup>5</sup>Department of Medical Genetics, Faculty of Medical Sciences, Tarbiat Modares University, Tehran, Iran

*Received June 13, 2022; revised September 25, 2022; accepted February 22, 2023*

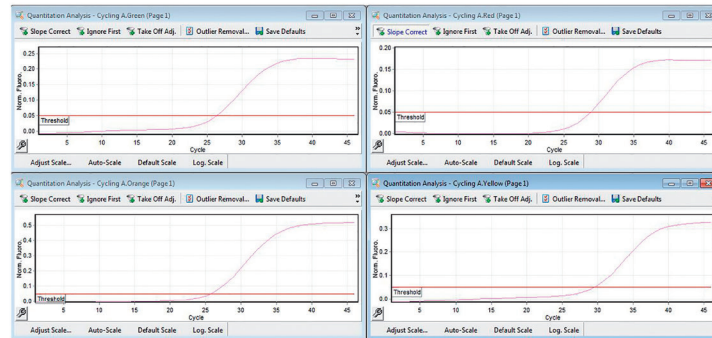
## (a) alpha



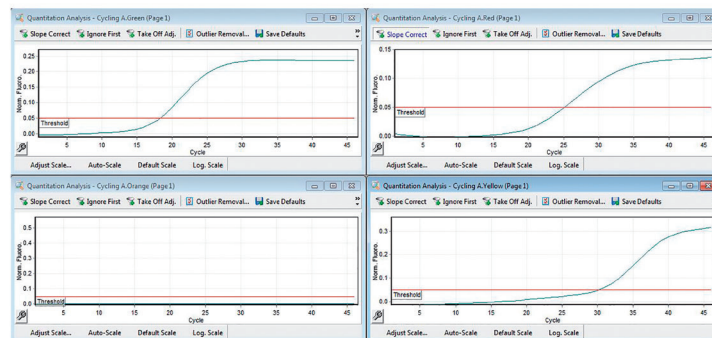
## (b) beta/gamma/lambda



## (c) delta



## (d) omicron

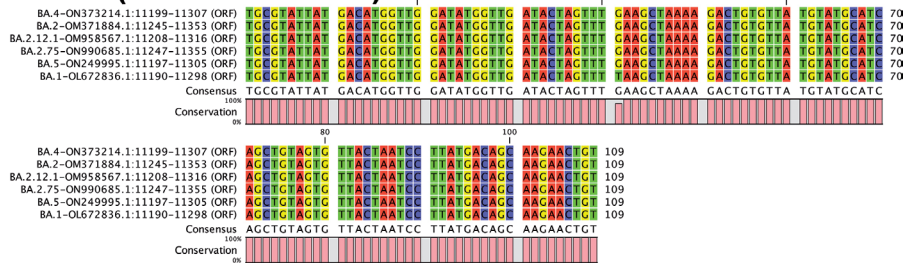


Supplementary Fig. 1

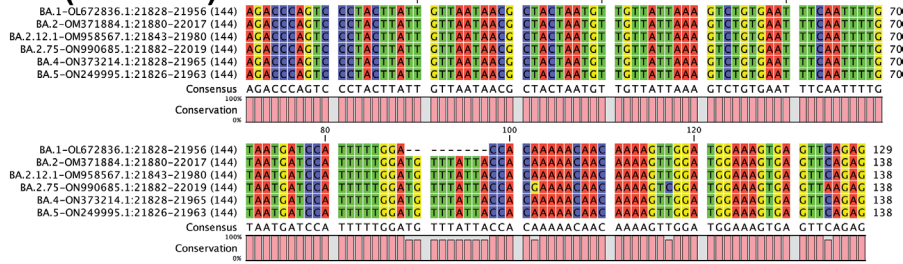
## Detection of SARS-CoV-2 variants by a commercial kit

(a) Amplification curve on the green (FAM) channel represented the alpha variant. (b) Amplification curves both on the green (FAM) and orange (TEXAS Red) channels represented either beta, gamma, or lambda variants. (c) Amplification curves on green (FAM), orange (TEXAS Red), and red (Cy5) channels showed the delta variant. (d) Amplification curves on the green (FAM) in addition to the red (Cy5) channels were indicative of the omicron variant presence.

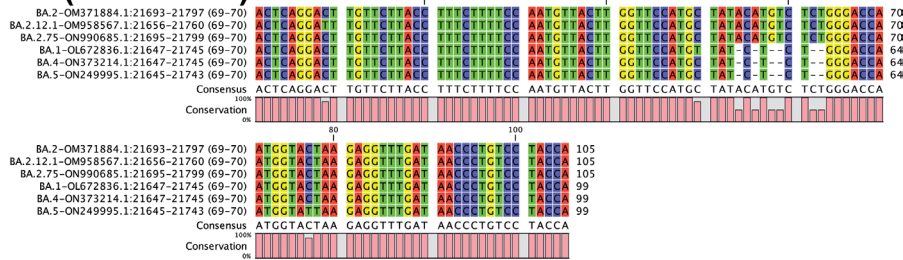
### NSP6 (DEL3675-3677)



### S1 (DEL144)



### S2 (DEL69-70)



Supplementary Fig. 2

Multiple sequence alignment of the target amplicons of primer set-1 (a), primer set-2 (b), and primer set-3 (c)